Functional silver-silicone-nanofilament-composite material for water disinfection

Meier, Margrith ; Suppiger, Angela ; Eberl, Leo ; Seeger, Stefan

Abstract: The roughness of superhydrophobic silicone nanofilaments (SNFs) is exploited to enlarge the contact area of conventional filter material. As an efficient wetting of the filter material is crucial for water treatment, the wettability of SNFs is readily modified from superhydrophobic to hydrophilic during the functionalization process. SNFs are coated on glass beads and subsequently modified with biocidal silver nanoparticles (AgNPs). The enlarged surface area of SNFs allows a 30 times higher loading of AgNPs in comparison to glass beads without SNF coating. Thus, in column experiments, the AgNP-SNF-nanocomposite-modified glass beads exert superior antibacterial activity towards suspensions of E. coli K12 compared to AgNP functionalized glass beads without SNFs. Additionally, reusing the AgNP-SNF-nanocomposite-coated glass beads with fresh bacteria contaminated medium increases their efficacy and reduces the colony forming units by ≈6 log units. Thereby, the silver loss during percolation is below 0.1 μg mL−1. These results highlight, first, the potential of AgNP-SNF-nanocomposite-modified glass beads as an effective filter substrate for water disinfection, and second, the efficiency of SNF coating in increasing the contact area of conventional filter material.

DOI: https://doi.org/10.1002/smll.201601072

Functional Silver-Silicone-Nanofilament-Composite Material for Water Disinfection

*Margrith Meier, Angela Suppiger, Leo Eberl, and Stefan Seeger**

The roughness of superhydrophobic silicone nanofilaments (SNFs) is exploited to enlarge the contact area of conventional filter material. As an efficient wetting of the filter material is crucial for water treatment, the wettability of SNFs is readily modified from superhydrophobic to hydrophilic during the functionalization process. SNFs are coated on glass beads and subsequently modified with biocidal silver nanoparticles (AgNPs). The enlarged surface area of SNFs allows a 30 times higher loading of AgNPs in comparison to glass beads without SNF coating. Thus, in column experiments, the AgNP-SNF-nanocomposite-modified glass beads exert superior antibacterial activity towards suspensions of E. coli K12 compared to AgNP functionalized glass beads without SNFs. Additionally, reusing the AgNP-SNF-nanocomposite-coated glass beads with fresh bacteria contaminated medium increases their efficacy and reduces the colony forming units by ≈6 log units. Thereby, the silver loss during percolation is below 0.1 μg mL^{-1}. These results highlight, first, the potential of AgNP-SNF-nanocomposite-modified glass beads as an effective filter substrate for water disinfection, and second, the efficiency of SNF coating in increasing the contact area of conventional filter material.

1. Introduction

Clean water is essential for the human health. However, the access to safe drinking water is not always ensured. One approach to overcome this problem is the application of point of use water filters. These small-scale water filters are of use in regions where centralized water treatment plants are not yet existing or unfeasible.[1] Point of use filters are also found in intensive care units of hospitals. Installed at the water tap outlet these filters prevent the distribution of pathogens via aerosols.[2] Such contaminated aerosols particularly endanger the health of immunosuppressed patients.

M. Meier, Prof. S. Seeger
Department of Chemistry
University of Zurich
Winterthurerstrasse 190, CH-8057 Zurich, Switzerland
E-mail: sseeger@chem.uzh.ch
A. Suppiger, Prof. L. Eberl
Department of Plant and Microbial Biology
University of Zurich
Zollikerstrasse 107, CH-8008 Zurich, Switzerland

DOI: 10.1002/smll.201601072

Nanomaterials for filter technology have aroused considerable attention in recent years.[3] A major advantage of nanomaterials lies in their large surface area per mass and volume, which implies an increased contact area of the medium being filtered per unit of filter volume. Materials used for water purification exhibiting a large contact area are, for example, nanoclays.[4] Another but less obvious group of materials for the application as filter substrate with a large contact area are superhydrophobic materials. By definition superhydrophobic surfaces possess a low surface free energy and a nanoscale roughness. This roughness accounts for the high surface area of these materials since the roughness is defined as the area ratio of the actual surface to the geometric flat surface with the same dimensions.[5,6] However, as superhydrophobic materials repel water little attention has been focused on these materials as high contact area material for water treatment. Nevertheless, if their wettability can readily be modified from superhydrophobic to hydrophilic, these materials become attractive for water purification. Silicone nanofilaments (SNFs) are such a superhydrophobic material.[7–9] Their wetting property is easily switched from superhydrophobic to hydrophilic by means of oxygen plasma.[10,11] Furthermore, recent investigations confirmed

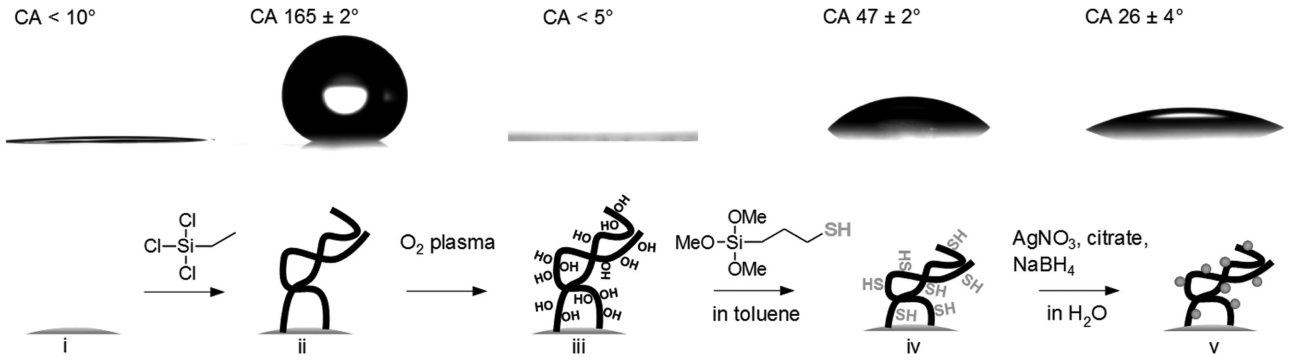

Figure 1. Reaction scheme of the different reaction steps for the preparation of AgNP-SNF-nanocomposite-coated glass beads. Above the reaction scheme, a water droplet on the respective smooth surface is depicted and the corresponding contact angle (CA) is stated.

the high surface area of the SNF coating.[12] This valuable feature led to various studies concerning SNFs as support material for catalysis and protein enrichment.[11,13] Hence, the high surface area likewise makes SNFs an appropriate candidate for the use as support material in water treatment. As SNFs grow as a fibrous coating on diverse substrates including glass, ceramics, cellulose, and metals, the filaments can be applied as support material on conventional filter substrates.[7,9] Furthermore, SNFs consist of silicone polymers which are known to be biocompatible and thermally as well as weathering stable.[14]

Silver nanoparticles (AgNPs) are frequently encountered as biocide in point of use water filters.[15–17] This is primarily owing to their broad biocidal activity combined with the relatively low toxicity to humans.[18] The antimicrobial activity of AgNPs is mainly based on the release of silver ions due to an oxidative dissolution process.[19–21] The silver ions may interact with functional groups present in cells such as thiols, phosphates and amines. However, the underlying cellular and molecular mechanisms, which in the end lead to cell death, are still not fully understood.[22–25] A main issue with nanoparticles in water disinfection is their dispersion and retention in the liquid media.[26] Immobilization of AgNPs on a filter material possessing a high surface area would allow for a high biocide loading. Moreover, since AgNPs are attached to the filter substrate, their retention is straightforward.

In this study, we show the efficacy of the SNF coating as a high surface area biocide support material applied on a conventional filter substrate. We use glass beads as the filter substrate on which the SNFs are grown. The SNFs serve as high surface area support for the biocidal AgNPs. The antibacterial activity of the AgNP-SNF-nanocomposite-coated glass beads are compared to pristine glass beads modified with AgNPs. As test organism for the effectiveness of the composite filter material we chose the Gram-negative bacterium *Escherichia coli* K12.

2. Results and Discussion

2.1. Wettability of the AgNP-SNF-Nanocomposite Coating

An efficient wetting of the filter substrate is essential for the formation of silver ions and thus for an effective antimicrobial activity.[20] In order to gain a comprehensive overview of the different surface wettabilities during the AgNP-SNF-nanocomposite preparation, the contact angle of each reaction step was measured. For the contact angle measurements, a flat surface was required, therefore glass slides instead of glass beads were coated according to the reaction scheme depicted in **Figure 1**. The cleaned glass surface (Figure 1i) was hydrophilic with a contact angle below 10°. After gas phase coating using trichloroethylsilane as precursor SNFs were formed on the surface (Figure 1ii). A drop of water put on the SNF-coated glass slide exhibited a contact angle of 165 ± 2°. The same drop rolled off from this superhydrophobic surface at an angle of 13 ± 2°. These contact and sliding angle values were in line with angles measured on SNF structures reported in previous studies.[7,27] Oxygen plasma treatment made the SNFs superhydrophilic with a water contact angle below 5° (Figure 1iii). This low contact angle indicated that the SNF surface was thoroughly hydroxylated. The thiol silanization with (3-mercaptopropyl)trimethoxysilane (MPTMS, Figure 1iv) increased the contact angle to 47 ± 2°. This result was about 10° lower than contact angles mentioned in literature for self-assembled layers of MPTMS on smooth surfaces.[28] One explanation for this deviation from literature values is the roughness induced by the SNF coating. This roughness potentially enhanced the hydrophilic property of the MPTMS surface.[5] The subsequent AgNP functionalization of the MPTMS-modified SNFs (Figure 1v) further lowered the contact angle to 26 ± 4°.

2.2. Preparation of AgNP-SNF-Nanocomposite-Coated Glass Beads

To obtain the SNF structure on glass beads trichloroethylsilane was used as precursor. The reaction was carried out in gas phase at a relative humidity of 43%. This coating procedure led to surfaces covered with a dense layer of entangled filaments as shown in the scanning electron microscopy (SEM) images in **Figure 2**a,b. In order to further functionalize the SNFs oxygen plasma was used to activate the surface. This plasma treatment introduces hydroxyl groups on the SNFs which serve as an anchor for linker molecules.[10,11] According to the hard–soft acid-base concept Ag^+ classified

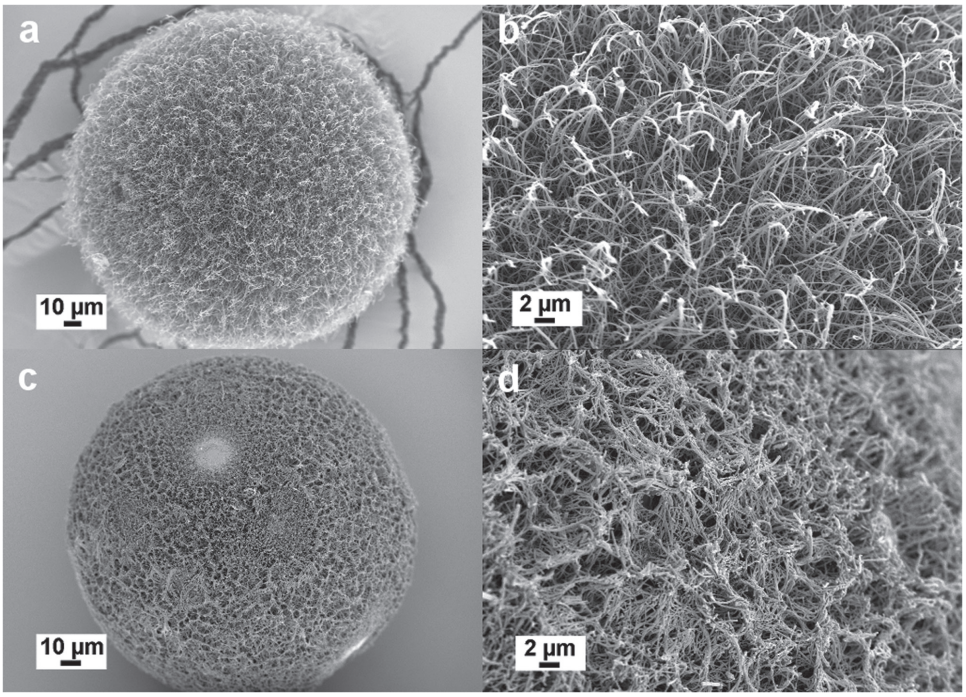

Figure 2. a,b) SEM images of SNF-coated glass beads. The glass beads are covered with a dense layer of SNF. c,d) SEM images of SNF-coated glass beads after modification with AgNPs. The loose structure of the SNF network has tightened together.

as a soft acid has a high affinity to sulfur which acts as a soft base.[29] Therefore, thiol groups were applied to immobilize AgNPs.[30] MPTMS was reacted with hydroxyl covered SNFs in toluene to create thiol groups on the surface. Thiols are sensitive to oxidation in air.[31] Thus, after cleaning procedure MPTMS-modified glass beads were immediately decorated with in situ prepared AgNPs. Silver nitrate was reduced to AgNPs by means of sodium borohydride as principal reducing agent and trisodium citrate as a stabilizer to prevent particle aggregation. These reagents were chosen for the AgNP preparation because they already demonstrated to yield small and antibacterial effective AgNPs elsewhere.[32,33] To minimize the risk of silver tarnishing, AgNP-SNF-nanocomposite-coated glass beads were stored under nitrogen atmosphere until further use in microbiological tests.[34]

During the MPTMS functionalization step, the upper ends of the anchored SNFs bundled together to form clusters. This bundle formation probably occurs due to capillary force and is also referred to as nanocarpet effect.[35] This nanocarpet effect presumably changed the morphology of the SNF layer. Figure 2c,d depicts such an altered SNF structure after functionalization with MPTMS and subsequent AgNP modification. The loose structure of the nanofilament network tightened together compared to the initial SNF coating. The coated glass bead in Figure 2c possesses round spots without SNFs. These round gaps emerged where glass beads touched the ground or each other during the coating process. Furthermore, SNFs could interlink glass beads in the close proximity which is shown in Figure S1 in the Supporting Information. However, gentle sieving through a sieve separated the glass beads from each other.

2.3. Characterization of AgNP-SNF-Nanocomposite-Coated Glass Beads

As the amount of immobilized AgNPs on the glass beads may crucially influence the biocidal activity, the silver content of the AgNP-SNF-nanocomposite-coated glass beads was determined by atomic absorption spectroscopy (AAS). The mass fraction of silver was 0.516 ± 0.011 wt‰ per mass of functionalized glass beads. This value was compared to the silver content of pristine glass beads modified with AgNPs which were prepared in an analogous manner to the AgNP-SNF-nanocomposite-coated glass beads, except that the SNF coating was omitted. Figure S2 in the Supporting Information depicts an SEM image of such AgNP-modified glass beads. The silver mass fraction of these AgNP-modified glass beads was found to be 0.017 ± 0.001 wt‰ per mass functionalized glass beads. Hence, if SNFs were used as support material for AgNPs the amount of immobilized silver was greatly improved, yielding in a 30-fold increase compared to non-SNF-coated glass beads. This significant difference also became apparent in the color of the silver functionalized glass beads. The AgNP-SNF-nanocomposite-coated glass beads exhibited a dark brown color whereas the AgNP-modified glass beads had a light yellow color as shown in the photograph in Figure S3 in the Supporting Information.

AgNPs deposited on silica powder was reported to yield a silver loading of 0.096 wt‰ per mass of silica powder, whereas the deposition of AgNPs on porous silica beads led to a silver content of 3.8 wt‰ per mass of silica beads.[17,36] Comparing these values with the silver loading of AgNP-SNF-nanocomposite-coated glass beads shows that the silver loading of AgNP-SNF-nanocomposite-coated glass beads is higher than the loading of AgNPs on silica powder but

inferior to the silver loading obtained on porous silica beads. This finding is no surprise as the coating thickness of SNFs is small compared to the diameter of the glass beads (≈10 µm compared to 150–212 µm). Consequently, the quasi-porous structure introduced by the SNF coating is restricted to the thin SNF layer on the surface.

To verify the formation of AgNPs on SNFs, the silver functionalized nanofilaments were investigated with transmission electron microscopy (TEM). The TEM image in **Figure 3**a shows an example of an SNF segment which was functionalized with AgNPs. The AgNPs are evenly distributed on the filament. Furthermore, the particle diameter distribution illustrated in Figure 3b revealed that most of the AgNPs had a diameter of 8.6 ± 3.5 nm. Even though around 6% of the AgNPs possessed a diameter larger than 15 nm. And it cannot be excluded that some of the large AgNPs detached during the ultrasonic treatment for TEM sample preparation. Silver ions are assumed to largely contribute to the biocidal activity of AgNPs.[21,23] Since the release of silver ions increases with increasing surface area,[37] smaller nanoparticles possess enhanced antimicrobial activity.[38,39] Moreover, Ivask et al. demonstrated that 10 nm AgNPs were more biocidal than predicted from the silver ion dissolution.[39] They explained the raise in toxicity for 10 nm AgNPs with an improved cellular bioavailability of silver.

Additionally, a selected area electron diffraction (SAED) pattern was recorded from AgNPs on an SNF. The SAED pattern in Figure 3c shows diffuse diffraction rings which suggested the formation of crystalline AgNPs. The diffraction rings possess spacing values of 1.2 Å (311), 1.4 Å (220), 2.0 Å (200), and 2.3 Å (111). These spacing distances are consistent with SAED diffraction pattern obtained for nanoparticles with a silver face centered cubic structure.[40] To exclude the formation of a silver thin film on the SNFs, energy dispersive X-ray (EDX) spectra were recorded from the black particles and the gray filaments depicted in the TEM image in Figure 3a. The EDX spectra in Figure 3d show that the nanoparticles contained silver (black spectrum "AgNP/SNF") whereas the filament (gray spectrum "SNF") gave no detectable silver signal. The silicon and oxygen signal originated from SNFs. The carbon signal might arise from ethyl groups present in SNFs and the formvar/carbon film-coated copper grid. The copper grid and TEM sample holder were responsible for copper signals. EDX analysis clearly confirmed that the silver was present in nanoparticulate form on SNFs.

2.4. Bacterial Tests

The antibacterial activity of coated glass beads was evaluated in column experiments against *Escherichia coli* K12. *E. coli* K12 is a Gram-negative bacterium that is commonly used as a model organism to investigate silver toxicity.[19,41] The glass beads were packed in mini-columns and a bacterial cell suspension with an OD_{600} of 0.1 or 1.0 (corresponding to ≈3×10^7 CFU mL^{-1} or 4×10^8 CFU mL^{-1}) in 0.9% NaCl was passed through with contact times of about 3 s or 30 min, respectively. The effluent was collected and dilutions were

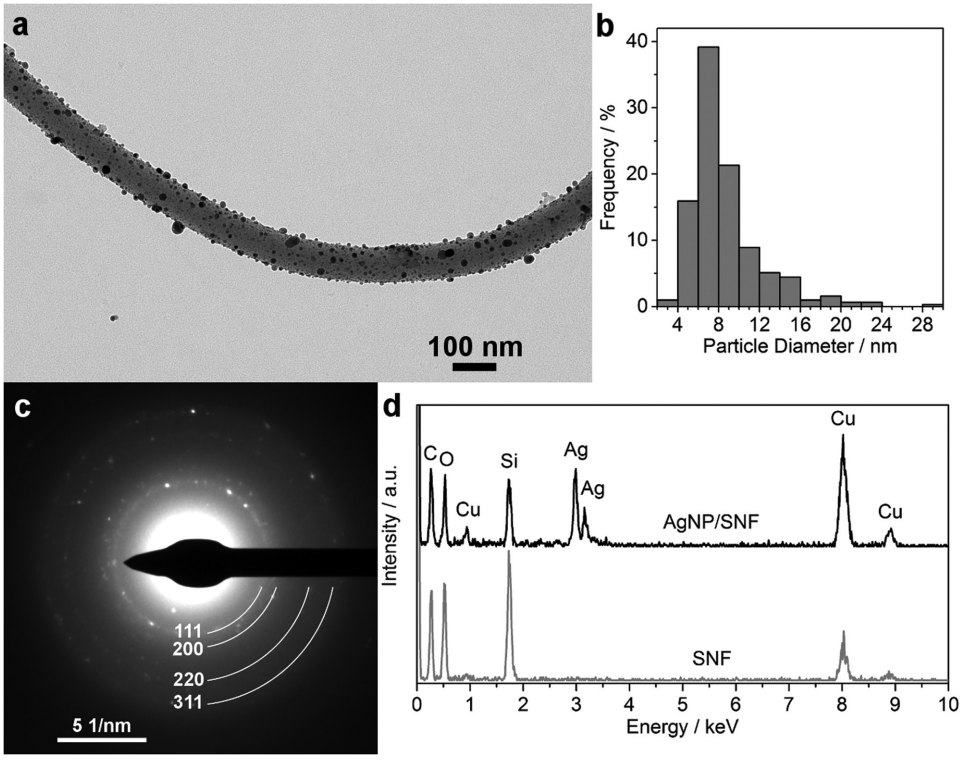

Figure 3. a) TEM image of an SNF modified with AgNPs. The AgNPs are evenly distributed on the filament. b) Particle diameter distribution of the AgNPs on SNFs. The AgNP diameter is 8.6 ± 3.5 nm. c) SAED pattern of AgNPs on an SNF. The SAED diffraction pattern corresponds to nanoparticles with an FCC structure. d) EDX spectrum of a spot on an SNF with AgNPs ("AgNP/SNF" black line) and EDX spectrum of a spot without AgNPs taken from the same SNF ("SNF" gray line). EDX analysis confirms the formation of AgNPs on SNFs.

Table 1. Overview of antibacterial test results for two types of silver-modified glass beads. Mini-columns were packed with either AgNP-modified glass beads (AgNP-GB) or AgNP-SNF-nanocomposite-coated glass beads (AgNP-SNF-GB). *E. coli* K12 suspension (OD_{600} 0.1 or 1.0) was passed through the mini-columns with contact times of about 3 s or 30 min. Antibacterial activity is indicated in percent and log reduction. Pristine glass beads were used as control. The column named "Usage mini-column" indicates how often the same mini-column filled with functionalized glass beads was used to disinfect fresh *E. coli* K12 contaminated medium within 48 h.

				E. coli K12 reduction			
	E. coli K12 load			AgNP-GB		AgNP-SNF-GB	
Retention time	OD_{600}	[CFU mL^{-1}]	Usage mini-column	log reduction	[%]	log reduction	[%]
3 s	0.1	3×10^7	1×	0.6	72	1	91
30 min	1.0	4×10^8	1×	≈0.3	≈50	2	99
30 min	1.0	4×10^8	3×	1	90	6	>99.999

spread on LB plates. Colony forming units (CFUs) were determined 24 h after incubation at 37 °C. A reduction of CFUs was observed with AgNP-SNF-nanocomposite-coated glass beads and AgNP-modified glass beads, while pristine glass beads or SNF-coated glass beads functionalized with the thiol linker MPTMS (MPTMS-SNF-coated glass beads, corresponding to reaction step iv in Figure 1) did not exhibit any antimicrobial effect under the conditions used. The representative LB plates depicted in Figure S4 in the Supporting Information show approximately the same number of CFUs for pristine and MPTMS-SNF-coated glass beads. This result suggests that bacteria are not clogging the filamentous structure of the SNF coating. Antimicrobial test results of the two different types of silver-modified glass beads are summarized in **Table 1** and **Figure 4**. With columns containing AgNP-SNF-nanocomposite-coated glass beads a contact time of about 3 s was sufficient to observe strong antibacterial activity. They exhibited a 91% reduction of CFUs in comparison to pristine glass beads. Whereas under the same conditions the AgNP-modified glass beads reduced the CFUs only to 72%. Figure 4a illustrates this result with representative LB plates. This biocidal effect is expected, as soluble species of silver are well known for their antimicrobial activity.[24,25,42,43]

However, upon increasing the bacterial load to an OD_{600} of 1.0 and extending the contact time to 30 min a more efficient bacterial inhibition was observed with the AgNP-SNF-nanocomposite-coated glass beads and to a lesser degree for the AgNP-modified glass beads. Figure 4b depicts corresponding LB plates from experiments with high bacterial loads. While the LB plate labelled with AgNP-GB (containing the effluent of AgNP-modified glass beads) shows an uncountably high number of CFUs, the LB plate labelled with AgNP-SNF-GB (containing the effluent of AgNP-SNF-nanocomposite-coated glass beads) exhibits a reduced number of CFUs. The AgNP-SNF-nanocomposite-coated glass beads reduced the CFUs to ≈99%, whereas for AgNP-modified glass beads the reduction of CFUs was estimated to be about 50%. Bacteria growth inhibition was determined based on rough visual inspection, as described in the Experimental Section.

It has been reported previously that storage of AgNPs in aqueous environment under aerobic conditions results in a higher antibacterial toxicity.[19] The increased toxicity is attributed to the oxidation of elemental silver to silver oxide which facilitates the release of silver ions into the medium.[19,20,44] This process would be beneficial for a point of use water filter as upon storage under moist conditions the thereby formed oxidized silver enhances the efficiency of the filter substrate. To validate this assumption, we exposed the columns after usage to air at room temperature without drying the substrate. The antibacterial activity of each column was retested after 24 and 48 h storage by adding fresh bacterial contaminated medium. The antibacterial effect of the AgNP-SNF-nanocomposite-coated glass beads increased steadily over time. Using this column, an ≈4 log reduction was observed after the second usage of the mini-column and after the third usage an ≈6 log reduction was achieved (>99.999% reduction in CFUs), depicted with representative LB plates in Figure 4c. An enhanced antibacterial activity was also observed for the AgNP-modified glass beads. Nevertheless, toxicity of these glass beads only increased after three usages to ≈90% (corresponding to an ≈1 log reduction).

The mass of silver in absolute number for a mini-column filled with 0.7 g AgNP-SNF-nanocomposite-coated glass beads was 361 ± 8 µg whereas 0.7 g AgNP-modified glass beads were loaded with 12 ± 1 µg silver. The obtained results demonstrated that this difference in silver mass played a role for efficient reduction of different bacterial loads under different retention times. Nevertheless, the 1 mL columns filled with 0.7 g filter substrate as used in our proof of principle experiments are not the ideal containers for a point of use water filter since the bacteria were not reliably killed. We observed considerable variations between experiments. A larger column could increase the contact time of the medium with the substrate, and therefore lead to more consistent antibacterial efficacy. However, a limitation of using a larger column in this experiment was that the filter substrate could only be prepared in small amounts.

A comparison of the antibacterial activity of the presented filter substrate with published data is difficult as no standardized protocol for the evaluation of the antibacterial performance is used in literature. However, considering the different bacterial load, the contact time, the amount of filter substrate filled in the column as well as the amount of silver immobilized on the AgNP-SNF-nanocomposite-coated glass beads the antibacterial activity of AgNP-SNF- nanocomposite-coated glass beads is comparable with published data of similar silver containing materials.[16,36,45]

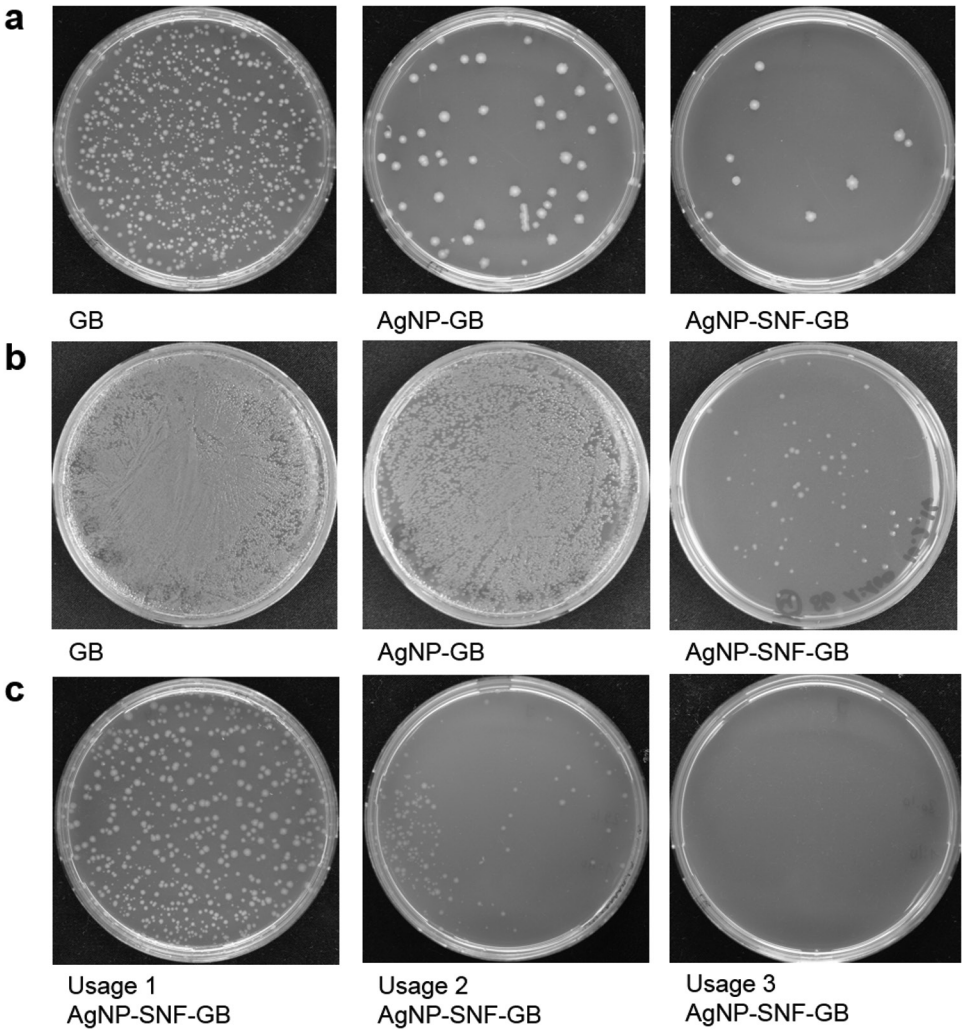

Figure 4. a) Silver-modified glass beads show antibacterial activity after a contact time of about 3 s. *E. coli* K12 (OD_{600} = 0.1) were added to the columns filled with pristine glass beads (GB), AgNP-modified glass beads (AgNP-GB) or AgNP-SNF-nanocomposite-coated glass beads (AgNP-SNF-GB). Shown are representative plates of 1:200 diluted effluent after overnight incubation at 37 °C. b) AgNP-SNF-nanocomposite-coated glass beads are more effective than AgNP-modified glass beads against high bacteria loads. The antibacterial activity of the glass beads was tested against *E. coli* K12 (OD_{600} of 1.0) after exposure to the respective glass beads for 30 min. Shown are representative plates of 1:200 diluted effluent collected from columns packed with pristine glass beads (GB), AgNP-modified glass beads (AgNP-SNF) or AgNP-SNF-nanocomposite-coated glass beads (AgNP-SNF-GB). c) Survival of *E. coli* K12 upon exposure to AgNP-SNF-nanocomposite-coated glass beads after 1, 2, or 3 usages. The mini-columns were used three times within 48 h to disinfect fresh *E. coli* K12 contaminated medium. For each plate, a 1:20 dilution of the effluent is shown after overnight incubation at 37 °C.

2.5. Substrate Leaching

According to the guidelines for drinking water quality as defined by the World Health Organization, the silver concentration in the effluent should not exceed 0.1 µg mL^{-1}. This amount of silver in potable water is considered as uncritical for human health.[46] In order to ensure that the silver functionalized glass beads satisfy this requirement, the silver concentration in the effluent was analyzed. To simulate comparable conditions during the leaching experiments as applied during the column experiments, 0.9% NaCl solution was used as the medium to be filtered. Furthermore, the medium was passed through the filter with a contact time of about 3 s. The silver concentration in the effluent of AgNP-SNF-nanocomposite-coated glass beads was below the significant detection limit of the ICP-MS instrument which is 0.1 ng mL^{-1}. Likewise, the silver dissolution of the AgNP-modified glass beads under the same conditions did not reveal a significant silver concentration.

Although NaCl forms the poorly soluble silver chloride (AgCl) with silver ions, the reported solubility of AgCl in water at 25 °C is 1.9 µg mL^{-1}.[47] Furthermore, depending on the Cl^-/Ag^+ molar ratio different species of soluble $AgCl_x^{(x-1)-}$ are formed.[43] Thus, the absence of silver in the effluent is not the result of a too low solubility of precipitated silver salts. Therefore, the contact time was extended to 24 h in order to obtain a detectable silver concentration. The silver content in the effluent per gram of AgNP-SNF-nanocomposite-coated glass beads was 0.13 ± 0.01 µg mL^{-1}, while the silver concentration in the effluent per gram of AgNP-modified glass beads was 0.07 ± 0.01 µg mL^{-1} after a contact time of 24 h. Considering the initial silver content

of the two different types of silver functionalized glass beads (516 ± 11 µg per gram AgNP-SNF-nanocomposite-coated glass beads and 17 ± 1 µg per gram AgNP-modified glass beads) silver leaching proceeds more readily in case of AgNP-modified glass beads. This finding suggests that the quasi-porous structure introduced by the SNF coating on the surface of AgNP-SNF-nanocomposite-coated glass beads may improve the silver retention. The silver concentration in the effluent calculated for mini-columns filled with 0.7 g AgNP-SNF-nanocomposite-coated glass beads as used in the bacterial tests is 0.09 ± 0.01 µg mL^{-1}. Consequently, even after a contact time of 24 h the silver concentration in the effluent meets the guidelines for drinking water quality.

After short contact times, silver-modified filter substrates showed distinct antimicrobial activity, even though in all tested effluents low silver concentrations were measured. Therefore, the antibacterial activity might depend on direct interaction of *E. coli* K12 with immobilized AgNPs. In literature, a more pronounced stress response in *E. coli* K12 was reported when AgNPs instead of an equivalent amount of silver ions were used. This observation was explained with a possibly increased dissolution of AgNPs in contact with the cell membrane due to an enhanced electrochemical potential.[48] Furthermore, the silver ion release is a complex process that depends on several factors such as pH, temperature, and chemical composition of the medium. In this respect, bacteria present in the medium can locally decrease the pH which promotes silver dissolution.[20,22]

Slowly washed out AgNPs are requirement for the reuse of a point of use water filter. Thus, the improved silver retention and the scarce silver ion concentration in the effluent are additional indications that AgNP-SNF-nanocomposite-coated glass beads can be reused several times. Nevertheless, as in the applied method only solutes were reliably detected, the presence of a minor number of SNF fragments in the effluent cannot be excluded.

3. Conclusion

An antibacterial surface coating based on SNFs functionalized with in situ prepared AgNPs was successfully synthesized. This newly created composite material was coated on glass beads which were used as filter substrate in column experiments. The comparison of the silver loading on SNF and non-SNF-coated glass beads clearly demonstrated the advantageous effect of SNFs regarding the surface area. The 30-fold increase in silver loading compared to glass beads without SNF coating allowed a superior antibacterial efficiency towards *E. coli* K12. The toxicity towards *E. coli* K12 after reuse of the silver functionalized glass beads with fresh bacteria contaminated medium increased while their silver loss was below 0.1 µg mL^{-1}. This finding suggests that AgNP-SNF-nanocomposite-coated glass beads are a potential filter substrate that could be reused several times. Moreover, considering their chemically inert nature and high loading capacity, SNFs are a viable and promising high surface biocide support material. Hence, SNFs could also be used as support material for other biocides. Additionally, the coating of various filter substrates such as fiberglass could be envisaged to adapt the filter performance for different purposes.

4. Experimental Section

Materials: Trichloroethylsilane (≥97%, Merck) and (3-mercaptopropyl)trimethoxysilane (MPTMS, 95%, Sigma–Aldrich) were stored and handled under nitrogen atmosphere. Anhydrous toluene (synthesis grade, Fisher Scientific), silver nitrate ($AgNO_3$, 99.85%, Acros Organics), trisodium citrate (>99.5%, Fluka), sodium borohydride ($NaBH_4$, ≥98%, Sigma–Aldrich) and nitric acid 70% (HNO_3, 99.999%, Sigma–Aldrich) were used as received. Glass beads (acid-washed) with diameter of 150–212 µm were purchased from Sigma–Aldrich. The diameter of the glass beads according to the manufacturer was verified by SEM. Figure S5 in the Supporting Information shows such glass beads.

Preparation of Silver-Nanoparticle-Modified Glass Beads: Two different types of silver-nanoparticle-modified glass beads were prepared namely AgNP-SNF-nanocomposite-coated glass beads and AgNP-modified glass beads. The preparation of AgNP-SNF-nanocomposite-coated glass beads included the following described reaction steps: silicone nanofilament coating, MPTMS functionalization and silver nanoparticle functionalization. The reaction steps were performed in the same order as listed. The preparation of the AgNP-modified glass beads included the following described reaction steps: MPTMS functionalization and silver nanoparticle functionalization. The reaction steps were performed in the same order as listed.

Silicone Nanofilament Coating: Acid washed glass beads (1.2 ± 0.2 g) were dispersed on an inlaid weighing paper in a polystyrene petri dish (diameter 60 mm). 6 petri dishes were put in a desiccator (volume 6.5 L). The relative humidity in the sealed desiccator was adjusted to 43% by flushing dry and wet nitrogen for 1 h. Afterwards, the gas phase coating was started by injecting trichloroethylsilane (1.5 mL, 11.4 mmol) through a septum on a watch glass which was placed on a 10 cm high glass stand in the middle of the desiccator chamber. The gas phase coating was carried out for 4 h at room temperature. The coated glass beads stick loosely together and form clusters of several millimeters in dimension. Therefore, these clusters were mechanically separated by a sieve with a mesh size of 0.85 mm.

MPTMS Functionalization: First, the surface of the glass beads was hydroxylated by oxygen plasma treatment (power 100 W, 5 min) in a low pressure plasma generator (Femto, Diener Electronic, Germany). The activated glass beads were immersed in a vial filled with anhydrous toluene (15 mL, 60–100 ppm water content) and MPTMS (150 µL, 0.8 mmol) was added. The glass beads were left in the sealed reaction vial for 23 h at room temperature. Afterwards, the glass beads were filtered and washed with ethanol and bidistilled H_2O.

Silver Nanoparticle Functionalization: AgNPs were prepared according to a modified protocol of Pallavicini et al.[32] The MPTMS-modified glass beads were put in a 200 mL Erlenmeyer flask with a 5 cm opening. Then, Millipore H_2O (100 mL) was added and the reaction mixture was cooled by means of an ice bath. Next, cooled 60 mM $AgNO_3$ solution (1 mL, 101 mg, 0.6 mmol in 10 mL Millipore H_2O), cooled 34 mM trisodium citrate solution (1.75 mL, 201 mg, 0.7 mmol in 20 mL Millipore H_2O), and cooled 20 mM $NaBH_4$

solution (0.75 mL, 75 mg, 2.0 mmol in 100 mL Millipore H_2O) were added in that order under stirring using an overhead stirrer. The stirring was continued for another 1 min. The glass beads were left in the AgNP colloid for 24 h at room temperature. Afterwards, the glass beads were filtered and washed with bidistilled H_2O. The glass beads were dried in air and stored under nitrogen atmosphere until further use.

Electron Microscopy: TEM, SAED, and EDX analysis were performed on a Tecnai G2 Spirit (FEI, The Netherlands) at 120 kV. Samples for TEM analysis were prepared by ultrasonicating SNF-coated glass beads functionalized with AgNP in ethanol (1 mL) for 1 min. Subsequently, some drops of the dispersion were put on formvar/carbon film-coated copper grid and dried in air. Particle size distribution was derived from several TEM images considering more than 600 particles measured using ImageJ 1.48v software (National Institutes of Health, USA). The SEM samples were sputtered with 15 nm platinum. The SEM images were recorded on a Zeiss Supra 50 VP (Zeiss, Germany) at 2 kV using the inlens detector.

Silver Content Determination: The silver content of the coated glass beads was measured with flame atomic absorption spectroscopy (F-AAS) in 0.2 M HNO_3 using an AA240FS spectrometer (Agilent Technologies, Switzerland). The F-AAS experiments were performed three times and measured in quintuplicate. The samples for the F-AAS experiments were digested in HNO_3 prior to the measurements. Hereto, the AgNP decorated glass beads were added in a test tube filled with 0.2 M HNO_3. The sealed test tube was put in a water bath at 85 °C for 48 h. Afterwards, the supernatant was filtered through a syringe filter with 0.2 µm pore diameter. The silver content of the effluent was measured with inductively coupled plasma mass spectrometry (ICP-MS). ICP-MS measurements were performed using an Agilent QQQ 8800 Triple quad ICP-MS spectrometer (Agilent Technologies, Switzerland) with standard x-lens setting, nickel cones and a "micro-mist" quartz nebulizer. Values reported are the average of 50 sweeps × 5 replicates. Coated glass beads (0.80 g) were filled in a 1 mL mini-column fitted with a 35 µm pore size filter at the outlet (mobicols, Life Systems Design AG, Switzerland). Prior to the effluent collection the glass beads were washed with Millipore H_2O (1 mL). Afterwards, effluent sample collection was done with 0.9% (w/v) NaCl solution (3 mL). The fluid was let through the filter with contact time of about 3 s. The effluent was acidified with concentrated HNO_3 to yield a 2% (v/v) HNO_3 solution. For the silver leaching tests with contact time of 24 h the coated glass beads were filled in a 15 mL polypropylene conical centrifuge tube to which 0.9% (w/v) NaCl solution (3 mL) was added. After 24 h contact time the supernatant was filtered through a syringe filter with 0.2 µm pore diameter and acidified with concentrated HNO_3 to yield a 2% (v/v) HNO_3 solution.

Contact and Sliding Angle Measurments: Contact angle measurements were performed on a contact angle system OCA (Dataphysics, Germany). A 10 µL droplet of Millipore H_2O was placed onto the respective surface. The contact angle of the drop was analyzed at five different positions on each sample using SCA software (Dataphysics, Germany). The sliding angles were measured on a custom-made tilting device. The microscope glass slides (Menzel Gläser, Germany) were coated following the above mentioned protocol for the glass beads. However, reaction vessels and sample holder were adapted to glass slides. For the MPTMS functionalization other quantities of chemicals were used. Furthermore, the reaction was carried out in a custom made reaction vessel. The reaction vessel was filled with anhydrous toluene (100 mL) and sealed. Afterwards, MPTMS (1 mL, 5.3 mmol) was added through a septum.

Antibacterial Tests: To 1 mL mini-columns (mobicols with two different screw caps, Life Systems Design AG, Switzerland) containing a 35 µm pore size filter (Life Systems Design AG, Switzerland) 0.7 g of the respective glass beads were added. An overnight culture in LB (Difco, Becton Dickinson, Switzerland) of *E. coli* K12 was harvested, washed with 0.9% NaCl and adjusted to an OD_{600} of 0.1 (corresponding to $\approx 3 \times 10^7$ CFU mL^{-1}) or 1.0 (corresponding to $\approx 4 \times 10^8$ CFU mL^{-1}). Samples of this cell suspension (130 µL) were added batchwise to the mini-column filled with the glass beads and incubated for 3 s or 30 min. Following incubation, the cell suspension was extruded and serial dilutions were spread on LB plates and incubated overnight at 37 °C for visual inspection. The columns were stored at room temperature. For tests with reused columns the same procedure was repeated after 24 and 48 h. Instead of adding new beads to the column, the same column which was stored at room temperature overnight was used. All tests were repeated five times in independent experiments of which at least three were considered for antibacterial test results. The log reduction was calculated based on the observed CFU mL^{-1} on LB plates using the formula: log reduction = $\log_{10}$ (A/B) with A = CFU mL^{-1} of pristine glass beads treatment and B = CFU mL^{-1} of AgNP-SNF beads treatment; the CFU mL^{-1} of the outlet with pristine glass beads was estimated based on the influent and the observed CFUs on LB agar plates. The percent reduction of CFUs was calculated by the formula (1 − [CFU of functionalized glass beads/CFU of pristine glass beads]) × 100.

Supporting Information

Supporting Information is available from the Wiley Online Library or from the author.

Acknowledgements

The authors are grateful to the Forschungskredit of the University of Zurich for financial support (grant no. FK-14-084). The authors thank Dr. Katsiaryna Tarasava and Jovana Jakovleska for measuring AAS and Dr. Ferdinand Wild for measuring ICP-MS. They also thank Dr. Georg Artus for constructive discussions and Dr. Georg Meseck for the glass bead coating protocol as well as helpful comments. They thank Isabell Scholl and Victoria Widrig for technical support. The center of microscopy and image analysis of the University of Zurich is gratefully acknowledged for providing their facilities.

[1] M. D. Sobsey, C. E. Stauber, L. M. Casanova, J. M. Brown, M. A. Elliott, *Environ. Sci. Technol.* **2008**, *42*, 4261.
[2] R.-P. Vonberg, T. Eckmanns, J. Bruderek, H. Rüden, P. Gastmeier, *J. Hosp. Infect.* **2005**, *60*, 159.
[3] X. Qu, J. Brame, Q. Li, P. J. J. Alvarez, *Acc. Chem. Res.* **2013**, *46*, 834.

[4] R. Srinivasan, *Adv. Mater. Sci. Eng.* **2011**, *2011*, 1.
[5] R. N. Wenzel, *Ind. Eng. Chem.* **1936**, *28*, 988.
[6] a) A. B. D. Cassie, S. Baxter, *Trans. Faraday Soc.* **1944**, *40*, 546; b) R. N. Wenzel, *J. Phys. Chem.* **1949**, *53*, 1466.
[7] G. R. J. Artus, S. Jung, J. Zimmermann, H.-P. Gautschi, K. Marquardt, S. Seeger, *Adv. Mater.* **2006**, *18*, 2758.
[8] a) J. Zhang, S. Seeger, *Angew. Chem.* **2011**, *123*, 6782; b) J. Zhang, S. Seeger, *Angew. Chem. Int. Ed.* **2011**, *50*, 6652; c) G. R. J. Artus, S. Jung, J. Zimmermann, S. Seeger, Superhydrophobic Coating, EP20030405455, WO2004113456; **2004**.
[9] G. R. J. Artus, S. Seeger, *Adv. Colloid Interface Sci.* **2014**, *209*, 144.
[10] J. Zimmermann, M. Rabe, G. R. J. Artus, S. Seeger, *Soft Matter* **2008**, *4*, 450.
[11] J. Zimmermann, M. Rabe, D. Verdes, S. Seeger, *Langmuir* **2008**, *24*, 1053.
[12] G. R. Meseck, A. Käch, S. Seeger, *J. Phys. Chem. C* **2014**, *118*, 24967.
[13] a) G. R. Meseck, R. Kontic, G. R. Patzke, S. Seeger, *Adv. Funct. Mater.* **2012**, *22*, 4433; b) G. R. Meseck, E. Fabbri, T. J. Schmidt, S. Seeger, *Adv. Mater. Interfaces* **2015**, *2*, 1500216.
[14] a) H.-H. Moretto, M. Schulze, G. Wagner, *Ullmann's Encyclopedia of Industrial Chemistry*, Wiley-VCH, Weinheim, Germany, **2012**; b) E. G. Rochow, W. F. Gilliam, *J. Am. Chem. Soc.* **1941**, *63*, 798.
[15] a) P. Jain, T. Pradeep, *Biotechnol. Bioeng.* **2005**, *90*, 59; b) V. A. Oyanedel-Craver, J. A. Smith, *Environ. Sci. Technol.* **2008**, *42*, 927; c) Y. Lv, H. Liu, Z. Wang, S. Liu, L. Hao, Y. Sang, D. Liu, J. Wang, R. I. Boughton, *J. Memb. Sci.* **2009**, *331*, 50; d) T. A. Dankovich, D. G. Gray, *Environ. Sci. Technol.* **2011**, *45*, 1992; e) S. Lin, R. Huang, Y. Cheng, J. Liu, B. L. T. Lau, M. R. Wiesner, *Water Res.* **2013**, *47*, 3959.
[16] D. Gangadharan, K. Harshvardan, G. Gnanasekar, D. Dixit, K. M. Popat, P. S. Anand, *Water Res.* **2010**, *44*, 5481.
[17] D. V. Quang, P. B. Sarawade, S. J. Jeon, S. H. Kim, J.-K. Kim, Y. G. Chai, H. T. Kim, *Appl. Surf. Sci.* **2013**, *266*, 280.
[18] a) P. L. Drake, K. J. Hazelwood, *Ann. Occup. Hyg.* **2005**, *49*, 575; b) S. W. P. Wijnhoven, W. J. G. M. Peijnenburg, C. A. Herberts, W. I. Hagens, A. G. Oomen, E. H. W. Heugens, B. Roszek, J. Bisschops, I. Gosens, D. van de Meent, S. Dekkers, W. H . de Jong, M. van Zijverden, A. J. A. M. Sips, R. E. Geertsma, *Nanotoxicology* **2009**, *3*, 109; c) B. Nowack, H. F. Krug, M. Height, *Environ. Sci. Technol.* **2011**, *45*, 1177.
[19] Z.-m. Xiu, Q.-b. Zhang, H. L. Puppala, V. L. Colvin, P. J. J. Alvarez, *Nano Lett.* **2012**, *12*, 4271.
[20] J. Liu, R. H. Hurt, *Environ. Sci. Technol.* **2010**, *44*, 2169.
[21] V. de Matteis, M. A. Malvindi, A. Galeone, V. Brunetti, E. de Luca, S. Kote, P. Kshirsagar, S. Sabella, G. Bardi, P. P. Pompa, *Nanomedicine: NBM* **2015**, *11*, 731.
[22] L. Rizzello, P. P. Pompa, *Chem. Soc. Rev.* **2014**, *43*, 1501.
[23] B. Le Ouay, F. Stellacci, *Nano Today* **2015**, *10*, 339.
[24] S. Chernousova, M. Epple, *Angew. Chem. Int. Ed. Engl.* **2013**, *52*, 1636.
[25] S. Chernousova, M. Epple, *Angew. Chem.* **2013**, *125*, 1678.
[26] Q. Li, S. Mahendra, D. Y. Lyon, L. Brunet, M. V. Liga, D. Li, P. J. J. Alvarez, *Water Res.* **2008**, *42*, 4591.
[27] a) J. Zimmermann, G. R. J. Artus, S. Seeger, *J. Adhes. Sci. Technol.* **2008**, *22*, 251; b) G. R. J. Artus, S. Seeger, *Ind. Eng. Chem. Res.* **2012**, *51*, 2631.
[28] a) D. G. Kurth, T. Bein, *Langmuir* **1993**, *9*, 2965; b) J. Liu, V. Hlady, *Colloids Surf. B Biointerfaces* **1996**, *8*, 25; c) J. J. Senkevich, G.-R. Yang, T.-M. Lu, *Colloids. Surf. A Physicochem. Eng. Asp.* **2002**, *207*, 139; d) C. R. Vistas, A. C. Águas, G. N. Ferreira, *Appl. Surf. Sci.* **2013**, *286*, 314.
[29] R. G. Pearson, *J. Am. Chem. Soc.* **1963**, *85*, 3533.
[30] A. Ulman, *Chem. Rev.* **1996**, *96*, 1533.
[31] S. Patai, (Ed.) *The Chemistry of Functional Groups*, Wiley, London, **1974**.
[32] P. Pallavicini, A. Taglietti, G. Dacarro, Y. A. Diaz-Fernandez, M. Galli, P. Grisoli, M. Patrini, G. S. De Magistris, R. Zanoni, *J. Colloid Interface Sci.* **2010**, *350*, 110.
[33] S. Agnihotri, S. Mukherji, S. Mukherji, *RSC Adv.* **2014**, *4*, 3974.
[34] a) H. E. Bennett, *J. Appl. Phys.* **1969**, *40*, 3351; b) M. D. Mcmahon, R. Lopez, H. M. Meyer, L. C. Feldman, R. F. Haglund, *Appl. Phys. B* **2005**, *80*, 915; c) J. L. Elechiguerra, L. Larios-Lopez, C. Liu, D. Garcia-Gutierrez, A. Camacho-Bragado, M. J. Yacaman, *Chem. Mater.* **2005**, *17*, 6042.
[35] a) J. Bico, B. Roman, L. Moulin, A. Boudaoud, *Nature* **2004**, *432*, 690; b) J.-G. Fan, D. Dyer, G. Zhang, Y.-P. Zhao, *Nano Lett.* **2004**, *4*, 2133.
[36] P. Kumari, H. Rickard, P. Majewski, *J. Nanosci. Nanotechnol.* **2012**, *12*, 8001.
[37] R. Ma, C. Levard, S. M. Marinakos, Y. Cheng, J. Liu, F. M. Michel, G. E. Brown, G. V. Lowry, *Environ. Sci. Technol.* **2012**, *46*, 752.
[38] a) J. Liu, D. A. Sonshine, S. Shervani, R. H. Hurt, *ACS Nano* **2010**, *4*, 6903; b) C. R. Bowman, F. C. Bailey, M. Elrod-Erickson, A. M. Neigh, R. R. Otter, *Environ. Toxicol. Chem.* **2012**, *31*, 1793.
[39] A. Ivask, I. Kurvet, K. Kasemets, I. Blinova, V . Aruoja, S. Suppi, H. Vija, A. Käkinen, T. Titma, M. Heinlaan, M. Visnapuu, D. Koller, V. Kisand, A. Kahru, *PLoS One* **2014**, *9*, e102108.
[40] R. M. Stiger, S. Gorer, B. Craft, R. M. Penner, *Langmuir* **1999**, *15*, 790.
[41] C. Marambio-Jones, E. M. V. Hoek, *J. Nanopart. Res.* **2010**, *12*, 1531.
[42] I. Sondi, B. Salopek-Sondi, *J. Colloid Interface Sci.* **2004**, *275*, 177.
[43] C. Levard, S. Mitra, T. Yang, A. D. Jew, A. R. Badireddy, G. V. Lowry, G. E. Brown, *Environ. Sci. Technol.* **2013**, *47*, 5738.
[44] C. Levard, E. M. Hotze, G. V. Lowry, G. E. Brown, *Environ. Sci. Technol.* **2012**, *46*, 6900.
[45] D. V. Quang, P. B. Sarawade, A. Hilonga, J.-K. Kim, Y. G. Chai, S. H. Kim, J.-Y. Ryu, H. T. Kim, *Appl. Surf. Sci.* **2011**, *257*, 6963.
[46] World Health Organization (WHO), *Guidelines for Drinking-Water Quality*, World Health Organization, Geneva, **2011**.
[47] C. W. Davies, A. L. Jones, *Trans. Faraday Soc.* **1955**, *51*, 812.
[48] J. S. McQuillan, H. G. Infante, E. Stokes, A. M. Shaw, *Nanotoxicology* **2012**, *6*, 857.

Received: March 30, 2016
Revised: August 10, 2016
Published online: September 13, 2016

